RECONFIGURABLE WHEEL-LEGGED ROBOT

IVAN VIRGALA, LUBICA MIKOVA, TATIANA KELEMENOVA, MICHAL KELEMEN, ERIK PRADA, DARINA HRONCOVA, MARTIN VARGA

Technical University of Kosice, Faculty of Mechanial Engineering, Department of Mechatronics, Deartment of Biomedical Engineering and Measurement, Kosice, Slovakia

DOI : 10.17973/MMSJ.2020_06_2020027

e-mail: michal.kelemen@tuke.sk

The paper deals with the reconfigurable robot design. A robot should be able to locomote via using wheels on a smooth terrain and locomote via using legs on a rough terrain or if necessary also cross an obstacle. The transformation between legs and wheels is a suitable concept to an unknown environment with obstacles. Wheeled locomotion is better from the viewpoint of energy consumption. A design of a wheeled mode of the robot was the first part of the design. The design of a quarter model of the mobile robot in a legged mode has been also made. A position vector of an end point (wheel) has been determined via using the Denavit-Hartenberg principle. The realised model is used mainly for an experimental study of the reconfigurable robot designed principle. A locomotion strategy of the robot has been proposed.

KEYWORDS

legged locomotion, reconfigurable, robot, wheeled locomotion, mechanism.

1 INTRODUCTION

Service robots are frequently used for many tasks such as cutting of grass, vacuum cleaning, swimming pool cleaning, cleaning of the windows, etc. Also many dangerous applications need mobile robots e.g. pyrotechnic robots, robots for service in nuclear power plants, fire-fighting robots, etc. Military use is a special area, where robots can be used as a main device in future. Military application has been is also as an impulse for the research and design of service robots used also for non-military applications, e g. help for human.

If the application area contains many static or dynamic obstacles, then a reconfigurable mobile robot is the best concept. The main aim has been to design a robot which able to loco mote on wheels or legs with the possibility to make any transformation between these kinds of locomotion. The main robot key property requirements involve: low weight, carrying capacity, ability to cross obstacles, resistance to environment impacts, intelligent behaviour, simple and user friendly controlling, low energy consumption, simple application, etc. Wheeled and legged robots are frequently used types of robots. Consequently, the combination of these types is a perfect selection for the robot undercarriage. These facts have been the reason for the design of the reconfigurable mobile robot [Shakeri 1998, Huang 2003, Smrcek 2003, Novák 2005, Sadati 2006, Simsaj 2013, Dunbar 2017, Halluc 2017, Nemec 2017, Skating 2017].

Mars Pathfinder, a six-legged wheeled robot is used for Mars exploration. The undercarriage has a high manoeuvrability and ability to cross the terrain with unknown geophysical properties [Dunbar 2017].

Halluc II, a mobile robot has eight segments composed of wheels and legs for the locomotion on rough terrain. This robot can locomote using the three mode wheeled vehicle, insect, and mammal. The eight segments can be modified for legged or wheeled locomotion [Halluc 2017].

2 DESCRIPTION AND MODEL OF PROBLEM AREA

Obstacles are a normally existing entity in natural and also artificial environments. The primary aim of the robot is the successful overcoming the obstacles. This requirement has led to the concept of the transformation of a wheeled undercarriage to a legged undercarriage.

The robot will consist of chassis and legs connected through the coxa joints to the robot chassis. The legs will consist of upper and lower parts connected through the knee joints. Wheels driven with servos will be placed on the end of the legs. The legs will be packed under the chassis during the wheeled mode. After transformation, these legs will be unpacked and the wheels will be used as feet. Walking will be solved on the basis of a big mammal example.

The requirements for the robot design can be divided into several criteria:

- Energy criterion,
- Geometry criterion,
- Accuracy criterion,
- Economy criterion.

These aspects will be evaluated during the robot design and practical realisation. The mentioned problems can be modelled as “model of problem area” using the UML language (Fig. 1).

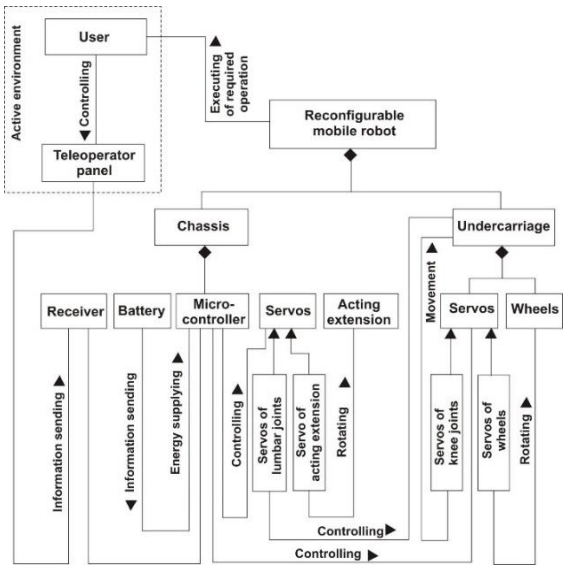

Figure 1. Model of problem area

The Unified Modelling Language (UML) is a general-purpose, developmental, modelling language in the field of software engineering, which is intended to provide a standard way to visualize the design of a system. UML was originally motivated by the desire to standardize the disparate notational systems and approaches to software design developed by Grady Booch, Ivar Jacobson and James Rumbaugh at Rational Software in 1994–1995, with further development led by them through 1996. In 1997 UML was adopted as a standard by the Object Management Group (OMG), and has been managed by this organization ever since.

In 2005 UML was also published by the International Organization for Standardization (ISO) as an approved ISO standard. Since then the standard has been periodically revised to cover the latest revision of UML [Booch 2005, ISO/IEC 19501 2005, ISO/IEC 19505 2012].

UML model (Fig. 1) shows that a user can communicate with the robot via using a communication panel. The communication panel is wirelessly connected with a robot microcontroller placed inside the robot chassis. The Microcontroller is able to directly control all servos in the robot. Every servo includes also potentiometer position sensors for ensuring the feedback information provided to the microcontroller. This feedback gives information about the current state of all legs.

3 DESIGN OF THE ROBOT CONCEPT

The design of the kinematic robot structure is shown in Figure 2. Unified kinematic symbols have been used for drawing the structure. The arrangement of front and back legs is the same. Upper parts of legs (3) are connected with the chassis (4) through the coxa joints (φ_{34}^{X} , φ_{34}^{Z}), which are able to rotate around X axis and Z axis. The lower parts of legs (2) are connected to the upper part of the legs (3) through the knee joints φ_{23}^{X}. The lower parts of legs include the parts φ_{12}^{Z}, which are able to rotate around Z axis and wheels are connected at these parts as end parts of the legs. Figure 4 shows that the width of the robot is twice larger than the upper parts of legs due to avoiding the collision of knee joints φ_{23}^{X} when they transform into the wheeled mode.

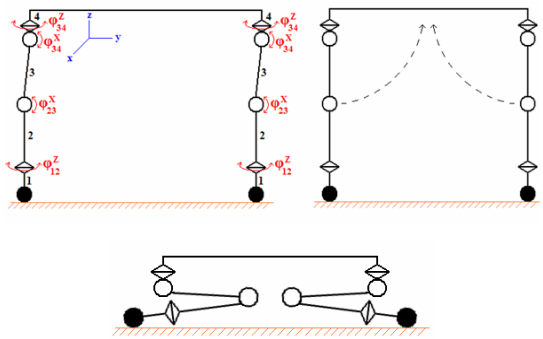

Figure 2. Design of robot kinematic structure

4 DESIGN OF THE WHEELED ROBOT MODE

The first step is the estimation of dimension (F
ig. 3) and gravitational forces for every part of the robot. The design assumes using the light weight material – polycarbonate (width 4mm) with the density $1.2 \cdot 10^{3} kg/m^{3}$, Young modulus $2300\, N/mm^{2}$. On the basis of the initial state design, the weights of robot´s parts have been estimated.

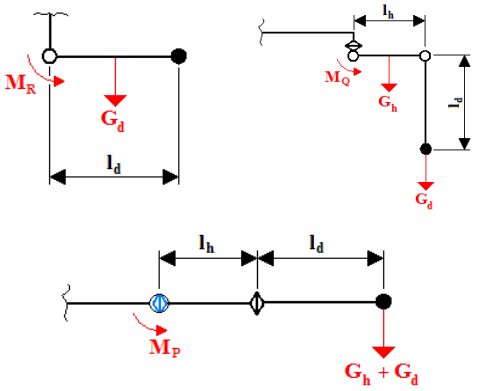

Figure 3. Loading of knee joint and coxa joint

Static analysis gives the approximation of the momentum in every joint. We assume an unfavourable position of the legs for counting of the momentum maximum value (Fig. 3). The maximum value of the momentum is when the legs are in the horizontal position.

The results from this analysis gave the estimation of momentum values. The results are necessary for selecting the servomechanisms. The servomechanism of HS-55 Micro Servo Motor has been selected for every joint as a unified actuator with stall momentum of 1.1 kg·cm.

$$O_f = f.G_{robota}^{výsl} \tag{1}$$

where *f* is a coefficient of the rolling resistance (for asphalt *f* is approx. 0.015), and $G_{robota}^{výsl}$ is an overall gravitational weight of the robot.

The road incline resistance can be obtained via using the equation:

$$O_s = G_{robota}^{výsl}.\sin\alpha \tag{2}$$

where α is an incline of the rolling plane and the reference ground (Fig. 4).

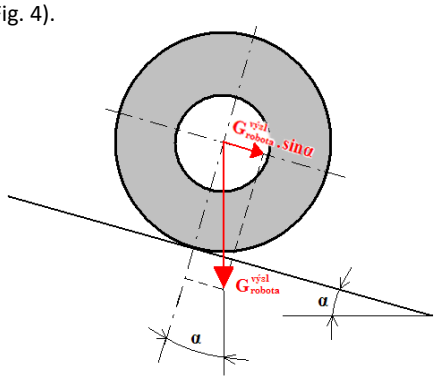

Figure 4. Road incline resistance

The acceleration resistance affects against the robot direction motion when the robot accelerates. It is described with the following equation:

$$O_z = \vartheta.m_{robota}^{výsl}.a_1 \tag{3}$$

where ϑ - coefficient for expressing the rotation part influence,

$m_{robota}^{výsl}$ - mass of robot

a_1 - acceleration of robot

The robot has also to solve the problems with obstacle avoidance, and obstacles can be of various characters. Overcoming the obstacle can be expressed by the resistance during overcoming the obstacle. The maximum height of an obstacle should be less than 1/3 of the robot´s wheel diameter (Fig. 5). It is also assumed that the wheels are still in contact with the ground. A successful obstacle overcoming is conditioned by the sufficient driving force and also coefficient of friction between the wheel and the obstacle edge. Obstacle overcoming can be supported also by using the locomoted robot kinetic energy.

The angle of the contact between the wheel and obstacle can be obtained from equation:

$$\sin\xi = \frac{d_w - 2.h}{d_w} \tag{4}$$

where d_w is a wheel diameter, h is a height of an obstacle. Distance from an obstacle can be solved as:

$$u = 0{,}5.\sqrt{d_w^2 - \left(d_w - 2.h\right)^2} \tag{5}$$

Consequently, it is possible to derive the obstacle overcoming resistance as:

$$O_p = \frac{G_{robota}^{výsl}.(l_{sf} + u).(\mu_\alpha - f).(f.\sin\xi + \cos\xi)}{(\cos\xi + f.\sin\xi - \mu_\alpha.\sin\xi).\left[h.(-\mu_\alpha + f) + 2.l_{sf} + u\right]} \tag{6}$$

where f is a friction coefficient, lsf is the dimension of the robot from the centre of gravity.

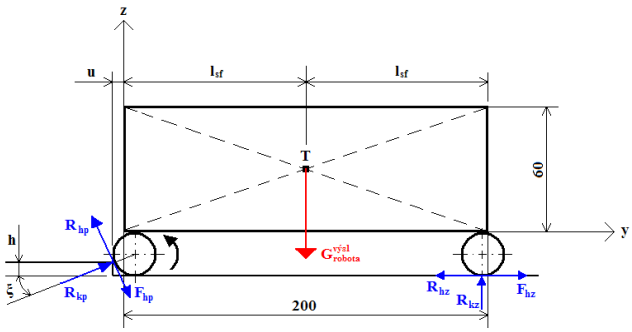

Figure 5. Obstacle overcoming resistance

Using the Newton's law, it is possible to derive the equation for the robot´s acceleration after 1m locomotion:

$$a_1 = \frac{F_H}{m_{robota}^{výsl}} - f.g \tag{7}$$

where F_H is a driving force, $m_{robota}^{výsl}$ is an overall weight of robot, f is a coefficient of the rolling resistance (f=0.015) and g is a gravitational acceleration (Fig. 6).

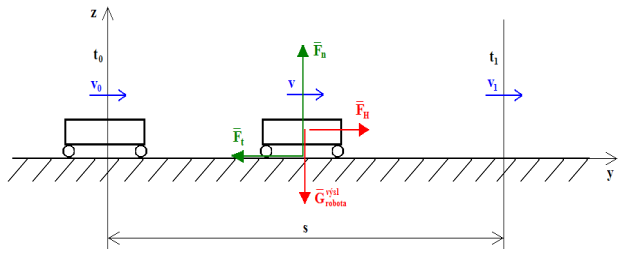

Figure 6. Robot locomotion in wheeled mode

After integration, the next equation shows the time needed for overcoming from one point to another (distance is 1m):

$$t_1 = \frac{v_1}{\frac{F_H}{m_{robota}^{výsl}} - f.g} = \frac{v_1}{a_1} \tag{8}$$

It is also possible to obtain the equation for a velocity after overcoming 1m of path:

$$v_1 = \sqrt{2.s.\left(\frac{F_H}{m_{robota}^{výsl}} - f.g\right)} \tag{9}$$

The driving force is given as a sum of all rolling resistances affecting against the robot´s locomotion:

$$F_H = O_f + O_s + O_z + O_p \tag{10}$$

The solution of equations (7) and (10) allows obtaining the equation for the driving force:

$$F_H = \frac{19.75 - f.g.m_{robota}^{výsl}.\vartheta}{1 - \vartheta} \tag{11}$$

F_H is a driving force on all wheels. If it is divided by 4 (number of driven wheels), it is the driving force per one wheel:

$$F_H^1 = \frac{F_H}{4} \tag{12}$$

The driving moment can be obtained via multiplying one wheel driving force F_H^1 by wheel radius r_w:

$$M_H^1 = F_H^1.r_w \tag{13}$$

This value is used for selecting a suitable driving motor.

5 DESIGN OF THE ROBOT´S LEGGED MODE

The aim is to determine the position vector of end point (wheel) via using the Denavit-Hartenberg principle. It has a matrix form:

$$A_i = \begin{bmatrix} \cos\delta_z & -\sin\delta_z.\cos\delta_x & \sin\delta_z.\sin\delta_x & X.\cos\delta_z \\ \sin\delta_z & \cos\delta_z.\cos\delta_x & -\cos\delta_z.\sin\delta_x & X.\sin\delta_z \\ 0 & \sin\delta_x & \cos\delta_x & Z \\ 0 & 0 & 0 & 1 \end{bmatrix} \tag{14}$$

δ_z - rotation around Z axis

δ_x - rotation around X axis

Z – displacement in Z axis

X – displacement in X axis

This method uses a principle which is based on moving and rotating local coordinate axes and consequential description of kinematics of every part. Positions will be written into a table form (Tab. 1). All legs are the same, so it is possible to make the analysis only for one leg. The solution is done for the front left leg. It means on quarter model of the robot´s legged mode (Fig. 7).

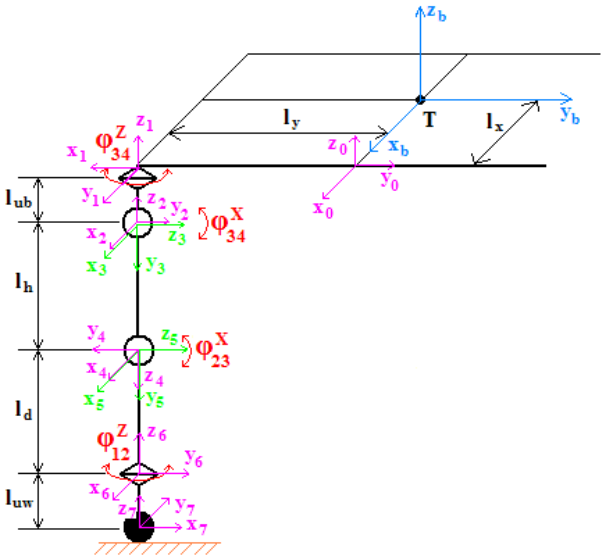

Figure 7. Quarter model of the mobile robot in legged mode

i	δz	Z	X	δx
0	0	0	lx	0
1	-π/2	0	ly	0
2	φ_{34}^{Z}	lub	0	0
3	0	0	0	π/2
4	0	lh	0	φ_{34}^{X}
5	0	0	0	π/2
6	0	ld	0	φ_{23}^{X}
7	φ_{12}^{Z}	luw	0	0

Table 1. Positions of local coordinates

After filling the values from Table 1 into the matrix (34), we obtain eight matrices, which will be multiplied with each other and the resulting matrix is in the form:

$$T_b^7 = \begin{bmatrix} A & D & G & r_x \\ B & E & H & r_y \\ C & F & I & r_z \\ 0 & 0 & 0 & 1 \end{bmatrix} \quad (15)$$

where:

$$A = \sin\varphi_{34}^{Z}.\cos\varphi_{12}^{Z} + \sin\varphi_{12}^{Z}.(-\cos\varphi_{34}^{Z}.\cos\varphi_{34}^{X}.\cos\varphi_{23}^{X} + \cos\varphi_{34}^{Z}.\sin\varphi_{34}^{X}.\sin\varphi_{23}^{X})$$

$$B = -\cos\varphi_{34}^{Z}.\cos\varphi_{12}^{Z} + \sin\varphi_{12}^{Z}.(-\sin\varphi_{34}^{Z}.\cos\varphi_{34}^{X}.\cos\varphi_{23}^{X} + \sin\varphi_{34}^{Z}.\sin\varphi_{34}^{X}.\sin\varphi_{23}^{X})$$

$$C = \sin\varphi_{12}^{Z}.(-\cos\varphi_{23}^{X}.\sin\varphi_{34}^{X} - \sin\varphi_{23}^{X}.\cos\varphi_{34}^{X})$$

$$D = -\sin\varphi_{34}^{Z}.\sin\varphi_{12}^{Z} + \cos\varphi_{12}^{Z}.(-\cos\varphi_{34}^{Z}.\cos\varphi_{34}^{X}.\cos\varphi_{23}^{X} + \cos\varphi_{34}^{Z}.\sin\varphi_{34}^{X}.\sin\varphi_{23}^{X})$$

$$E = \sin\varphi_{12}^{Z}.\cos\varphi_{34}^{Z} + \cos\varphi_{12}^{Z}.(-\sin\varphi_{34}^{Z}.\cos\varphi_{34}^{X}.\cos\varphi_{23}^{X} + \sin\varphi_{34}^{Z}.\sin\varphi_{34}^{X}.\sin\varphi_{23}^{X})$$

$$F = \cos\varphi_{12}^{Z}.(-\cos\varphi_{23}^{X}.\sin\varphi_{34}^{X} - \sin\varphi_{23}^{X}.\cos\varphi_{34}^{X})$$

$$G = \cos\varphi_{34}^{Z}.\cos\varphi_{34}^{X}.\sin\varphi_{23}^{X} + \cos\varphi_{34}^{Z}.\sin\varphi_{34}^{X}.\cos\varphi_{23}^{X}$$

$$H = \sin\varphi_{34}^{Z}.\sin\varphi_{34}^{X}.\cos\varphi_{23}^{X} + \sin\varphi_{34}^{Z}.\sin\varphi_{34}^{X}.\cos\varphi_{23}^{X}$$

$$I = \sin\varphi_{34}^{X}.\sin\varphi_{23}^{X} - \cos\varphi_{34}^{X}.\cos\varphi_{23}^{X}$$

$$r_x = l_{uw}.(\cos\varphi_{34}^{Z}.\cos\varphi_{34}^{X}.\sin\varphi_{23}^{X} + \cos\varphi_{34}^{Z}.\sin\varphi_{34}^{X}.\cos\varphi_{23}^{X}) + l_d.\cos\varphi_{34}^{Z}.\sin\varphi_{34}^{X} - l_h.\cos\varphi_{34}^{Z} + l_x$$

$$r_y = l_{uw}.(\sin\varphi_{34}^{Z}.\sin\varphi_{34}^{X}.\cos\varphi_{23}^{X} + \sin\varphi_{34}^{Z}.\sin\varphi_{34}^{X}.\cos\varphi_{23}^{X}) + l_d.\sin\varphi_{34}^{Z}.\sin\varphi_{34}^{X} - l_h.\sin\varphi_{34}^{Z} + l_y$$

The matrix (15) includes the searched position vector **r** (r_x, r_y, r_z) of the end point of the leg to start point of the coordinate system. The derivation of this vector is the vector of velocities **v** (v_x, v_y, v_z), and next derivation is the vector of accelerations **a** (a_x, a_y, a_z).

6 LOCOMOTION OF THE MOBILE ROBOT

The virtual model (Fig. 8) has been created for the locomotion analysis from the viewpoint of controlling. The wheeled mode is based on four wheels which are synchronised for forward locomotion. Change of wheel velocities can be used for changing the locomotion direction. Servomechanisms have been selected as a drive unit for the wheels.

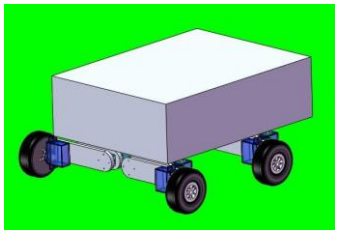

Figure 8. Mobile robot in wheeled mode

There is also is another way of changing the locomotion direction. The example of algorithms for turning to the left or right is shown in Figure 9. Coxa joint servomechanism has been used for turning to the left or right.

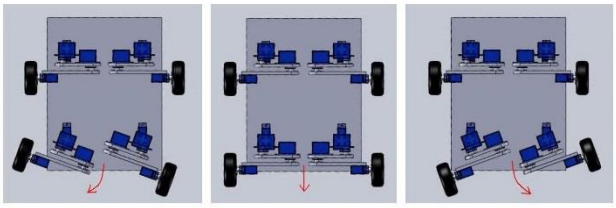

Figure 9. Mobile robot – locomotion direction change

Figure 10 shows the reconfiguration of the robot from the wheeled mode to the legged one. The transformation is executed through shifting the legs from the bottom side of undercarriage. This shifting will be ensured via rotating of coxa joint actuator and knee joint actuator. The same servomechanisms as for wheels are used also for the legs. The undercarriage will move high from the ground and the wheels are used as feet.

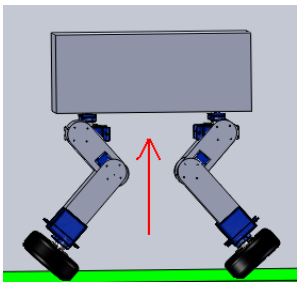

Figure 10. Robot reconfiguration from wheeled mode to legged mode

The legged locomotion of the robot is inspired by an elephant´s locomotion (Fig. 11). One leg is lifted up and the important task is to move the centre of gravity among other three legs.

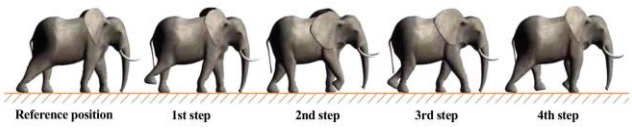

Figure 11. Elephant locomotion

Modified principle is also applied to the legged mode of the mobile robot (Fig. 12).

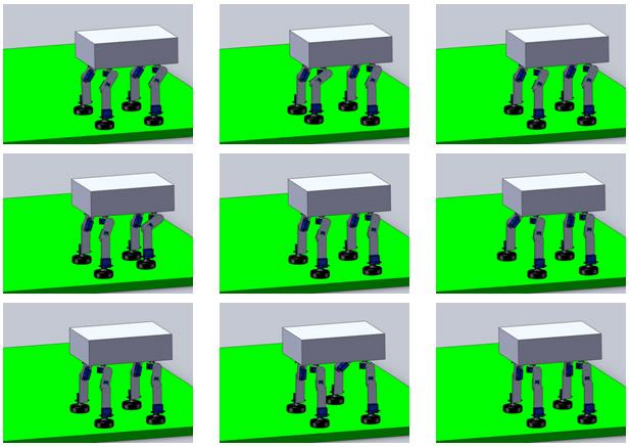

Figure 12. Sequence of legged locomotion

The realisation of the robot is shown in Figure 13. The control unit is composed from the microcontroller with supporting electronics. The robot is remotely controlled by an operator. The realised model is used mainly for an experimental study of the reconfigurable robot designed principle.

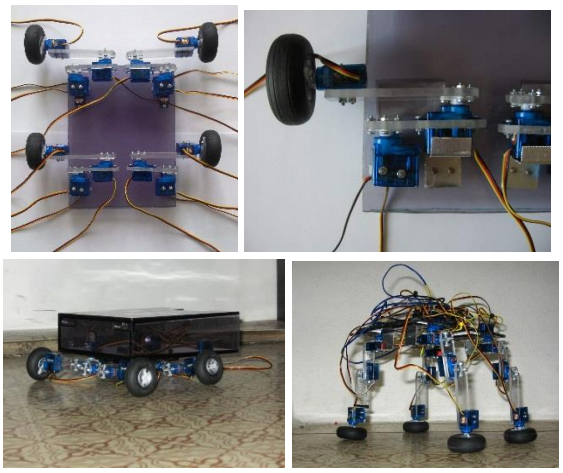

Figure 13. Realisation of the mobile robot

7 CONCLUSIONS

Numerous authors [Xing 2006, Koniar 2014, Karavaev 2016, Lipták 2016, Turygin 2016, Janos 2017, Kuric 2017, Simonova 2017, Komak 2018, Vysocky 2018, Mostyn 2020] also include selected problems from the field, and it is possible to use them as an inspiration for the tasks.

The paper is focused on designing the reconfigurable mobile robot, and a functional model was created after the large analysis. The first proposition comes from an early stage design process and it was analysed due to the need to identify the suitable drives for this robot. The analysis gave the kinematic quantities in joints of the robot and the information was used for selecting the drive. The next part deals with the mobility of robot and with the transformation to the locomotion modes. A functional prototype was created for the experimental simulation verification and analysis results.

The robot can be used mainly for application with various obstacles, where standard wheeled or legged locomotion is not effective. The selection of locomotion mode brings also lower energy consumption and higher time for using.

Future plans include several problems which came from the design of the robot. The problems will be the aim of our next scientific research as well as the development of a manipulation arm is planned as a future task.

ACKNOWLEDGMENTS

This work was supported partially by the VEGA Grant Agency, Slovak Ministry of Education, Grant VEGA 1/0389/18.

REFERENCES

[Booch 2005] Booch, G. et al. Unified Modeling Language User Guide, The (2 ed.). Addison-Wesley, 2005, 496 p. ISBN 0321267974.

[Dunbar 2017] Dunbar, B., Loff, S. Mars Pathfinder. Last Updated: 8-4-2017. Available online: <https://www.nasa.gov/mission_pages/mars-pathfinder>.

[Halluc 2017] Halluc II: 8-legged robot vehicle [online]. Last Updated: 17-9-2009. Available online: <http://pinktentacle.com/2007/07/halluc-ii-8-legged-robot-vehicle/>.

[Huang 2003] Huang, Y.J. Variable structure control for a two-link robot arm. Electrical Engineering, 2003, Vol. 85, Issue 4, pp. 195–204. https://doi.org/10.1007/s00202-003-0167-5.

[ISO/IEC 19501 2005] ISO/IEC 19501:2005 - Information technology - Open Distributed Processing - Unified Modeling Language (UML) Version 1.4.2. Iso.org. 2005-04-01. Retrieved 2015-05-07.

[ISO/IEC 19505 2012] ISO/IEC 19505-1:2012 - Information technology - Object Management Group Unified Modeling Language (OMG UML) - Part 1: Infrastructure. Iso.org. 2012-04-20. Retrieved 2014-04-10.

[Janos 2017] Janos, R. et al. Conceptual design of a leg-wheel chassis for rescue operations. International Journal of Advanced Robotic Systems, 2017, Vol. 14. Issue 6, pp. 1-9. https://doi.org/10.1177/1729881417743556.

[Karavaev 2016] Karavaev, Y.L., Kilin, A.A. Nonholonomic dynamics and control of a spherical robot with an internal omniwheel platform: Theory and experiments. Proceedings of the Steklov Institute of Mathematics, 2016, Vol. 295, Issue 1, pp. 158-167.

[Komak 2018] Komak, M. et al. The generation of robot effector trajectory avoiding obstacles. MM Science Journal, 2018, Vol. June, pp. 2367-2372.

[Koniar 2014] Koniar, D. et al. Virtual Instrumentation for Visual Inspection in Mechatronic Applications. In: Proc. 6th Conf. on Modelling of Mechanical and Mechatronic Systems (MMaMS). Vysoke Tatry, Slovakia, Nov 25-27, 2014.

[Kuric 2017] Kuric, I. et al. Development of simulation software for mobile robot path planning within multilayer map system based on metric and topological maps. International Journal of Advanced Robotic Systems, 2017, Vol. 14, Issue 6, pp. 1-14. https://doi.org/10.1177/1729881417743029.

[Liptak 2016] Lipták, T. et al. A geometric approach to modeling of four- and five-link planar snake-like robot. International Journal of Advanced Robotic Systems, 2016, Vol. 13, Issue 5, pp. 1-9. https://doi.org/10.1177/1729881416663714.

[Mostyn 2020] Mostyn, V. et al. Dimensional optimization of the robotic arm to reduce energy consumption. MM Science Journal, 2020, Vol. March, pp. 3745-3753.

[Nemec 2017] Nemec, D. et al. Control of the mobile robot by hand movement measured by inertial sensors. Electrical Engineering, 2017, Vol. 99, Issue 4, pp. 1161–1168, https://doi.org/10.1007/s00202-017-0614-3.

[Novak 2005] Novák, P. Mobile robots – drives, sensors, controll. BEN – Technical publication, Prague, 2005. ISBN 80-7300-141-1.

[Sadati 2006] Sadati, N., Babazadeh, A. Optimal control of robot manipulators with a new two-level gradient-based approach. Electrical Engineering, 2006, Vol. 88, Issue 5, pp. 383–393. https://doi.org/10.1007/s00202-005-0304-4.

[Shakeri 1998] Shakeri, A. A methodology for development of mechatronic systems. Ph.D. thesis. Norwegian University of Science and Technology, 1998. ISBN 82-471-0340-0.

[Simonova 2017] Simonova, A. et al. Uses of on-off controller for regulation of higher-order system in comparator mode. Electrical Engineering, 2017, Vol. 99, Issue 4, pp. 1367-1375. https://doi.org/10.1007/s00202-017-0610-7.

[Simsaj 2013] Simsaj, D. et al. Design of Two Legged Robot. American Journal of Mechanical Engineering, 2013, Vol. 1, Issue 7, pp. 355-360. ISSN 2328-4102.

[Skating 2017] Skating Robot 'Swims' on Land [online]. Last Updated: 8-6-2009. Available online: <http://gizmodo.com/296026/skating-robot-swims-on-land>.

[Smrcek 2003] Smrcek, J. et al. Some problems in design of wheeled mobile robot undercarriadge. Acta Mechanica Slovaca, 2003, Vol. 7, Issue 3. TU SjF Košice, pp. 129-136.

[Turygin 2016] Turygin, Y. et al. Enhancing the reliability of mobile robots control process via reverse validation. International Journal of Advanced Robotic Systems, 2016, Vol. 13, Issue 6, pp. 1-8. doi.org/10.1177/1729881416680521.

[Xing 2006] Xing, X.X. et al. Decentralized robust controller design for robots with torque saturation constraint. Electrical Engineering, 2006, Vol. 88, Issue 5, pp. 367–374. https://doi.org/10.1007/s00202-005-0295-1.

[Vysocky 2018] Vysocky, A., Novak, P. HUMAN – robot collaboration in industry. MM Science Journal, 2018, Vol. June, pp. 903-906.

CONTACTS:

Michal Kelemen, prof. Ing. PhD.
Technical University of Kosice, Faculty of Mechanical Engineering
Department of Mechatronics
Letna 9, 042 00 Kosice, Slovak Republic
michal.kelemen@tuke.sk